Use of Rheological and Other Data in Asphalt Engineering Problems

JOHN G. BRODNYAN, Research Engineer, Franklin Institute Laboratories, Philadelphia, Pa.

The performance in service of asphalts in various systems depends both on the influence to which the material is subjected and the intrinsic properties of the asphalt itself. A wide variety of asphalts has been investigated with respect to (a) their rheological behavior under both static and dynamic load, (b) their breaking properties, and (c) other properties such as water permeability, photochemical decomposition, etc.

The rheological data are condensed to generalized curves of both the dynamic storage and loss moduli versus frequency, the temperature dependence of these curves, and the dependence of the initial viscosity on temperature. By the use of the softening point and penetration, it is shown how, with the aid of the stated curves and empirical relationships, to find the whole rheological behavior of an asphalt.

Several prototype examples of engineering problems are solved, and are evidence that asphalts, no less than metals, can be dealt with as engineering materials. A flow problem is solved with the aid of the curves of initial viscosity versus temperature. Use of the two rheological moduli in solving engineering problems is shown for the case of the attenuation of vibrations. Also the method of extending classical elastic theory to these visco-elastic materials is outlined, with the particular case of a bending beam given in detail. Finally, the problem of whether thermal changes will cause cracking of an asphalt is investigated.

● THE performance in service of asphalts in various systems depends both on the influence to which the material is subjected and the intrinsic properties of the asphalt itself. A wide variety of asphalts have been investigated with respect to these properties: (a) their rheological behavior under both static and dynamic load, (b) their breaking properties, and (c) other properties such as water permeability, photochemical decomposition, etc.

The rheological data, obtained under the direction of W. Philippoff at The Franklin Institute, was condensed to generalized curves of both the dynamic storage and loss moduli versus frequency, the temperature dependence of these curves and the dependence of the initial viscosity on temperature. By the use of the softening point and penetration, it was shown how, with the aid of the stated curves and empirical relationships, to find the whole rheological behavior of an asphalt.

Several prototype examples of engineering problems were solved, and are evidence that asphalts, no less than metals, can be dealt with as engineering materials. A flow problem was solved with the aid of the curves of initial viscosity versus temperature. The use of the two rheological moduli in solving engineering problems was shown for the case of the attenuation of vibrations. Also the method of extending classical elastic theory to these visco-elastic materials was outlined, with the particular case of a bending beam given in detail. Finally the problem of whether thermal changes will cause cracking of an asphalt was investigated.

MATERIALS INVESTIGATED

The asphalts investigated were chosen to give as wide a variety as could be obtained. The conventional tests of these NARC asphalts, when they were received, are given in Table 1. Three years later, when A.S. Orr had the asphalts checked at Gulf Oil's Refinery Technology Laboratory in Philadelphia, most had not changed much, but the MD and GC asphalts had hardened significantly. The results of a Sternberg-Rostler (5) analysis provided by F.G. Gzemski of the Atlantic Refining Company are given in Table 2.

The gel asphalts were Mid-Continent air-blown stocks, the Medium asphalts were Venezuelan air-blown asphalts and the Sol asphalts were straight-run distilled residues from Santa Maria Valley, California crude, except that Sol D is propane extract asphalt from a different crude which is essentially the resin fraction alone.

The different types can be distinguished by their softening point—penetration ratios. If the log of the penetration for 100 g acting for 5 sec at 77 F is plotted against the softening point in degrees Fahrenheit straight lines (Fig. 1) with different slopes for each family are obtained.
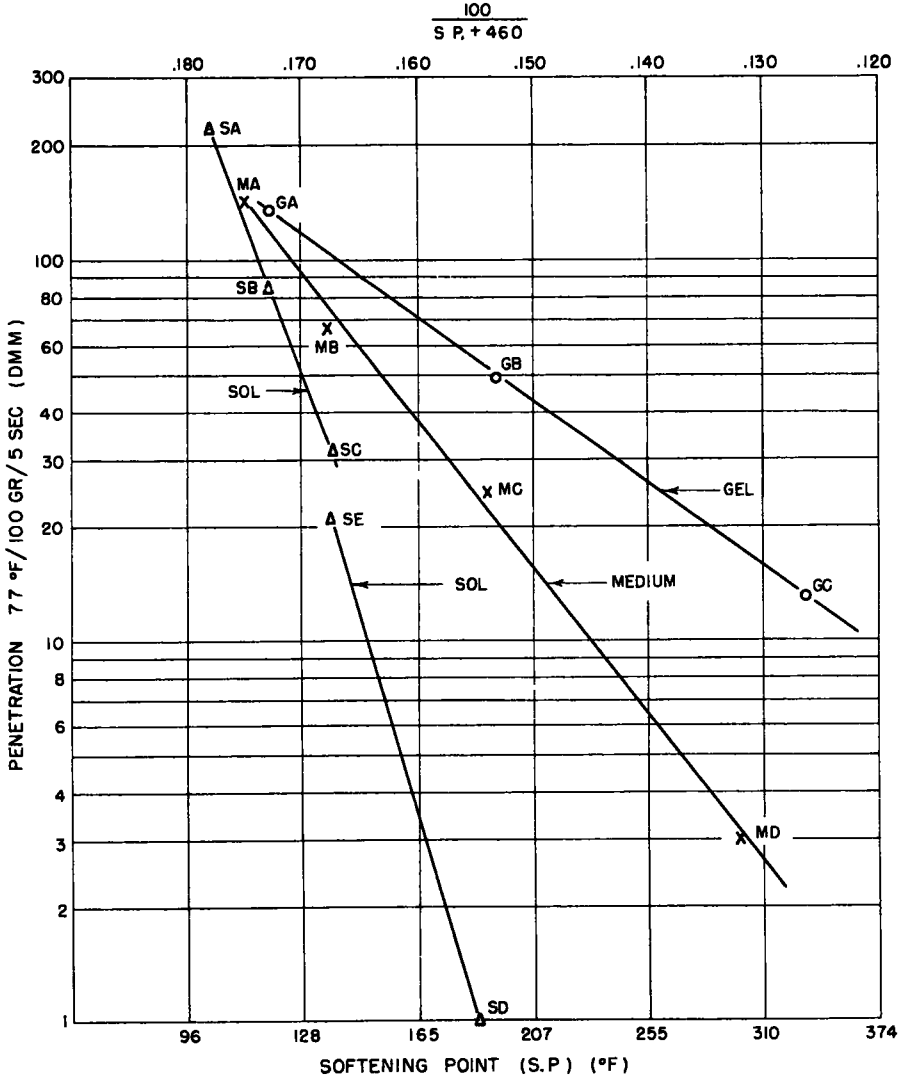

Figure 1. Softening point—penetration relationships of NARC standard asphalts (log penetration vs 100/(460 + softening point)).

EXPERIMENTAL METHODS AND RESULTS

Rheological Investigations

As asphalts are visco-elastic materials the mechanical behavior depends on the time of loading ("frequency" or rate of shear) and temperature. The usual viscous response

has been investigated by using a coni-cylindrical (rotational) viscometer described elsewhere (6) as well as a high-pressure capillary viscometer described in another publication (7). As asphalts are non-Newtonian liquids it was expected and proved, after an initial period of loading, during which the elastic strains are brought to equilibrium, their properties depend only on the rate of shear and not on the amount of shear. The dynamic properties have been investigated in The Franklin Institute's vibration tester which has been described by Philippoff (8). In this instrument a sinusoidal stress is imparted to a visco-elastic material and the deformation follows in a sinusoidal manner, but will lag

TABLE 1
IDENTIFICATION OF ASPHALTS

Code Name	Penetration Decimillimeters			ASTM	D 946-47T		Softening Point	Ductility (cm) ASTM D113-44	°F/cm/min	Flash Point ASTM D92-46 C.O.C. Fire Point		Loss on Heating 5 hr at 325 F	Penetration of Residue ASTM DG-39T	Solubility in CCl₄	Solubility in DS₂	Insoluble in n-hexane	Ash Content	Specific Gravity
	$\frac{32}{200}/60$	$\frac{77}{100}/5$	$\frac{115}{50}/5$	$\frac{115}{200}/5$	$\frac{150}{100}/5$	$\frac{185}{50}/5$	F	$\frac{77}{5}/1$	$\frac{39.2}{1}/1$	F	F	%	dmm.	%	%	%	%	
Gel A	77	135	301+	---	---	---	127	8.6	2.8	520	600	.036	134	99.6	---	18.5	.05	.977
Gel B	34	50	77	---	---	---	193	2.1	1.9	530	605	.016	51	99.6	---	25.5	.08	.983
Gel C	11	13	18	---	---	---	335	non-ductile		585	620	.004	14	99.4	---	36.4	.01	1.004
Med A	42	141	300+	---	---	---	112	150+	26.4	490	575	.054	109	99.8	---	22.5	.005	1.014
Med B	27	67	234	---	---	---	134	31.5	5.1	500	575	.052	50	99.8	---	27.0	.009	1.017
Med C	13	25	49	---	---	---	191	4	0.7	510	625	.038	16	99.8	---	35.1	.006	1.031
Med D	< 1	3	5	12	21-23	31	299	non-ductile		550	640	.0032	< 1	99.8	---	49.2	.009	1.057
Sol A	86	225	300+	---	---	---	102	150+	150+	365	455	1.015	94	99.9	---	28.4	.01	1.016
Sol B	31	85	300+	---	---	---	118	150+	150+	420	510	.334	60	99.9	---	23.7	.005	1.044
Sol C	16	32	114	---	---	---	137	104	1.1	480	570	.065	29	99.9	---	31.9	.015	1.045
Sol D	0	1	6	23	110	290+	184	non-ductile		695	755	0	< 1	99.8	---	18.1	.015	1.056
Sol E	1	21	168	---	---	---	137	---	---	---	---	---	---	----	---	----	---	1.039

behind the stress by an angle δ. The ratio of the maximum stress to the maximum strain gives the absolute value of the complex modulus $G^* = G' + iG''$ where $i = \sqrt{-1}$. The in-phase component of stress divided by the strain is called the storage modulus, G', because it is a measure of the energy stored. The component of the stress 90 deg out of phase divided by the strain is called the loss modulus, G'', because it is a measure of energy loss. By the methods of complex variables it can be shown that the following relationships hold true:

$$G' = |G^*| \cos \delta \qquad (1a)$$

$$G'' = |G^*| \sin \delta \qquad (1b)$$

$$|G^*| = \sqrt{(G')^2 + (G'')^2} \qquad (1c)$$

$$\frac{G''}{G'} = \tan \delta \qquad (1d)$$

This instrument gives both the complex modulus G^*, which is comparable to one-third the stiffness as defined by van der Poel, and the loss angle δ thereby enabling the separation of the complex modulus into G' and G'' which is related to the dynamic viscosity η by the relationship $G'' = \omega \eta'$ where ω is the circular frequency ($2\pi f$). The curves of G' and G'' give more information than the "stiffness" which is essentially an envelope of these two curves. Isothermal curves of the moduli, G' and G'', were obtained over

TABLE 2
STERNBERG-ROSTLER ANALYSIS OF NARC ASPHALTS

Code Name	Asphaltenes	N-Base Resins	Group 1 Resins	Group 2 Resins	Saturated Hydrocarbons
Gel A	17.0	12.3	13.5	26.9	30.3
Gel B	23.1	10.0	12.2	25.1	29.6
Gel C	33.3	5.0	13.7	21.1	27.0
Med A	18.1	18.4	15.6	28.8	19.1
Med B	20.2	19.7	16.0	27.4	16.8
Med C	29.3	14.5	14.8	24.2	17.1
Med D	42.8	12.3	12.6	21.3	11.0
Sol A	24.6	31.2	21.5	15.8	6.9
Sol C	21.9	36.9	21.4	14.5	5.4
Sol D	6.5	38.0	27.7	24.7	2.6

a wide range of temperatures and frequencies (Fig. 2) and were shifted together, using Ferry's method of reduced variables: (9) a superposition principle, which set up an equivalence between temperature and frequency, to obtain a large reduced curve (Fig. 3). The fundamental relationships of this method are:

$$G'(\omega) = \frac{T\rho}{T_o\rho_o} G'_o (\omega a_T) \qquad (2a)$$

$$G''(\omega) = \frac{T\rho}{T_o\rho_o} G''_o (\omega a_T) \qquad (2b)$$

$$\eta'(\omega) = a_T \left(\frac{T\rho}{T_o\rho_o}\right) \eta_o' (\omega a_T) \qquad (2c)$$

$$\eta = a_T \frac{T\rho}{T_o\rho_o} \eta_o \qquad (2d)$$

where the quantities without subscript refer to the absolute temperature T and those with subscript $_o$ refer to the reference temperature T_o. η' is the apparent viscosity and η is the initial viscosity, which is a constant; ρ is the density. The initial viscosity is the highest one exhibited by a non-Newtonian liquid and is at any given temperature found at lowest rates of shear or frequencies. It is seen that the function a_T gives essentially the temperature dependence of the initial viscosities.

TABLE 3
ASPHALT IMPACT TEST
1 in.-lb = 0.700 ergs/cm^2 x 10^6

Asphalt	Temperature F	Temperature C	Impact Energy (in.-lb) Uncorrected
Gel A	-20	-28.9	1.36 + .25
Gel C	-20	-28.9	1.39 + .25
Gel C	32	0	2.46 + .29
Med D	-20	-28.9	1.71 + .22
Med D	- 9	-22.8	1.63 + .12
Med D	80	26.7	1.80 + .32
Sol D	-20	-28.9	1.44 + .25
Sol D	80	26.7	1.38 + .25
Sol D	32	0	1.52 + .25

In practice, the isothermal curves of G' and G" versus frequency are plotted on a log-log scale. To reduce the curves, each pair of isothermal curves is first shifted vertically by the factor $\dfrac{T\rho}{T_0\rho_0}$ and then moved along the frequency axis by the same amount until the points line up with the reference curves (25 C) to give continuously smooth graphs. The amount of horizontal shift necessary to bring coincidence (log a_T) is a measure of the temperature dependence of the material. These shifts for asphalts are given as a function of temperature in Figure 4.

The method of reduced variables makes possible the reduction of the properties of visco-elastic bodies to only two general curves: (a) the dependence of G' and G" (or η') on the reduced frequency, and (b) the temperature dependence of log a_T. As the asphalt families react qualitatively in the same manner with only the time scale transposed, all the reduced curves have been superposed to give three generalized reduced curves, which were then combined to give one large curve with three "sections" (Fig. 5).

The validity of the method of reduced variables for asphalts has been checked by measuring the mechanical properties at 20 kilocycles with a torsion crystal arrangement.
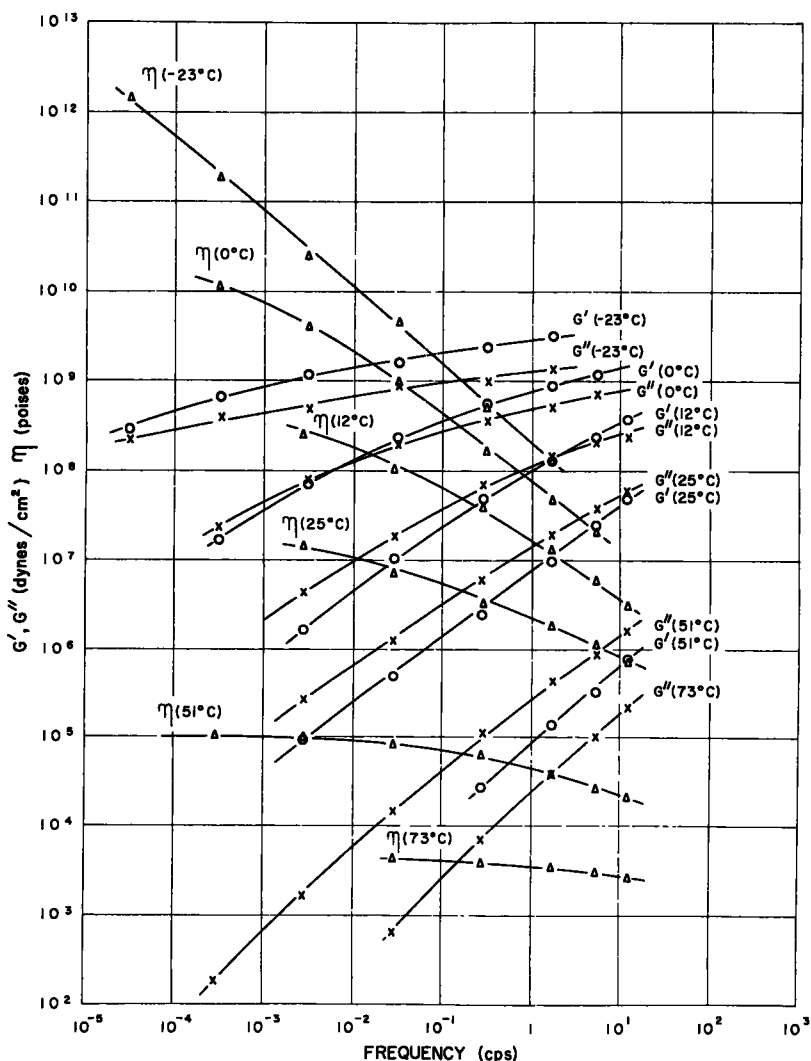

Figure 2. Mechanism of reduction (isotherms—Sol C asphalt).

This arrangement gave essentially the same values as reduced curves measured at much lower frequencies and temperatures. The validity of the method has also been checked with a solution of polyisobutylene (10).
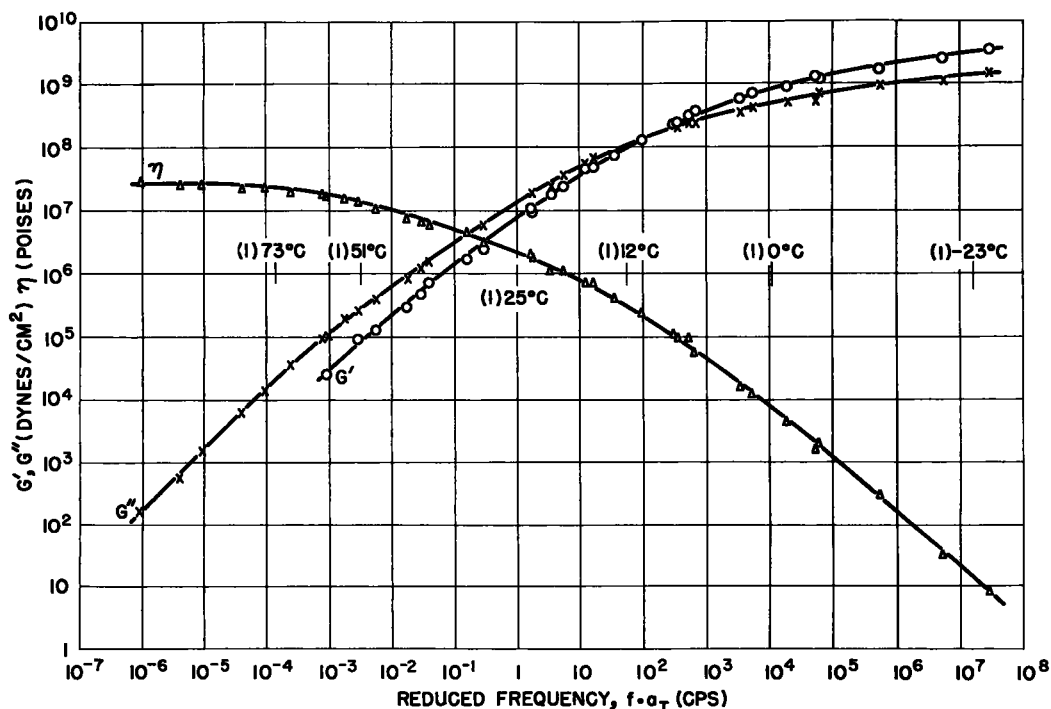

Figure 3. Mechanism of reduction (reduced curves—Sol C asphalt).

In addition, the steady state viscosity data has also been condensed. As the asphalts are non-Newtonian liquids, the viscosity varies with the rate of shear; but they behave like Newtonian bodies below a certain rate of shear; that is, they have a viscosity that is independent of both rate of shear and shearing stress. This is the initial viscosity defined earlier. Actually, it has been found that the upper limit for Newtonian behavior at low rates of shear is determined primarily by the shearing stress. The rate of shear is determined by the viscosity of the asphalt at that particular shearing stress (about $3,000$ dynes/cm^2). This initial viscosity has been plotted as function of temperature on a plot (Fig. 6) based on the empirical relationship of Walther; $\log \log (\nu + 0.8) = m \log T$, where ν is the kinematic viscosity and T the absolute temperature.

As the viscosity at very low frequencies is equal to this initial viscosity, by the use of the time-temperature reduced plots the initial viscosity at very low temperatures could be obtained by extrapolation and plotted as in Figure 6. This has been done to extend the initial viscosity data down to -23 C.

Recently it was shown experimentally (8) that the change in viscosity with rate of shear for visco-elastic bodies is very similar to the decrease of the viscosity with the circular frequency of vibration. This has also been shown to be true for asphalts. This means that, to a first approximation, rate of shear (D) and circular frequency ($\omega = 2\pi f$) can be interchanged.

Limited experience with coal tar and rubberized asphalt did not show any major qualitative departures from the behavior of the NARC normal asphalts.

The coal tar curves appeared to be similar to those for hard Sol asphalts, whereas the rubberized asphalts are typical of those for medium asphalts. Of course the properties of the rubberized asphalt may change with large changes in concentration and methods of incorporation and this would have to be ascertained by extensive experimentation.

An important consideration in engineering use is the effect of filler on the rheological behavior of asphalt. C. van der Poel (4) has found that the stiffness of an asphalt-mineral mixture is determined only by the stiffness of the asphalt alone since, by comparison, the filler is "infinitely" stiff and the volume concentration of the mineral aggregate. This is the same as the results of Nielsen, Wall and Richmond (11) on another visco-elastic material, polystyrene. They found that the storage modulus $\overline{G}'$ is approximately a linear function of the volume fraction up to at least 40 percent filler with mineral aggregates in polystyrene.

Breaking Properties and Impact Resistances of Asphalts

The breaking strength of asphalt is important as it limits the stresses that can be applied in use. The stresses may be limited in two ways: (a) if a certain stress is imposed, it must be less than the breaking stress, and (b) if a certain deformation in a given time is imposed, it must be less than the breaking stress divided by the stiffness at this rate of loading.

The second limitation assumes that there is a constant stiffness at a given rate of loading up to the point of fracture. It has been found experimentally that this linearity occurs up to the point where brittle fracture occurs.
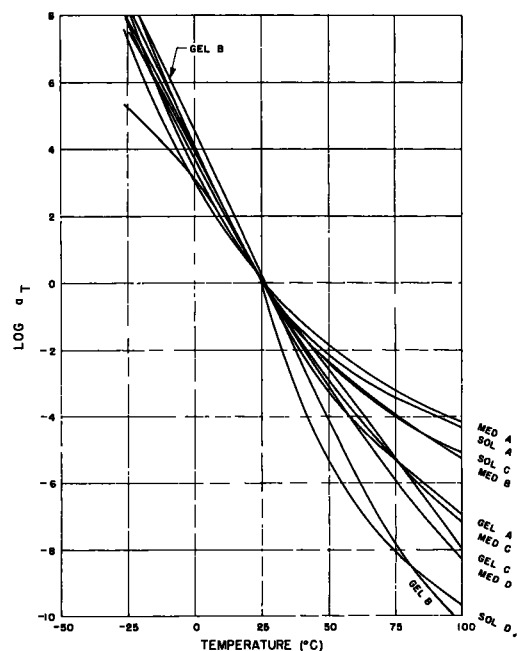

Figure 4. Temperature dependence of a_T values.

When asphalts are overloaded they fail in three different modes depending on the stress-strain, time and temperature conditions. It appears that when asphalts are essentially viscous, they fail in a ductile fashion; when essentially elastic, they exhibit brittle failure; and when their viscous and elastic responses are both important, they show a ragged break.

This indicates that the breaking strength cannot be taken to be a constant but is a function of time and temperature. This has been found experimentally. The dependence of breaking strengths on time is not as great as the dependence of the moduli G' and G'', on time and it appears to follow the reduced variable principle. At high rates or low temperatures the breaking stress is found to be $0.70 - 2.43 \times 10^7$ dynes/cm^2 and the deformation at break is found to go through a maximum.

In investigating the strength of films of asphalt, C. Mack (12) found that the film strength varied between 1.30 and 1.45 x 10^7 dynes/cm^2. It has been found, however, that the temperature dependence of the breaking strength is essentially the same as that of the non-destructive rheological behavior and accordingly composite curves could be formed for the breaking strength versus deformation rate similar to the ones of moduli versus frequency. This behavior is qualitatively like that of GR-S rubber as reported by T. L. Smith (13).

An important related phenomenon is that of impact resistance. The various asphalts were investigated with a Tinius Olsen Impact machine and the results are given in Table 3. The results show that the asphalts have very similar impact resistances which one would be led to believe from the similarity of the breaking properties.

In comparing two asphalts to see which would give the better impact resistance one finds that the one with the lower storage modulus and higher tan δ at the frequency of impact, approximately 10^2 to 10^3 cycles per sec, is the better.

Temperature Dependence of Asphalts

Since there is a similarity in shape between all the curves of G' and G" versus frequency they can be superimposed by shifting along the frequency axis. It is then natural to ask, are there some similarities between the temperature dependences, curves of log a_T vs temperature, which will enable a superposition of these curves. The answer is yes.

Recently, Williams, Landel and Ferry (14) have found that upon choosing suitably a separate reference temperature, T_S, for each individual polymer system, and expressing a_T as a function of $T - T_S$, this function turns out to be identical for a wide variety of polymers and their solutions. That a_T is a function of $T - T_S$ has also been found true for all the NARC asphalts over a wide range of temperatures. The reference temperature T_S was chosen arbitrarily for one system, 243 K for a high molecular weight polyisobutylene, the same as that taken by Ferry as a reference. The plots of log a_T versus T for the asphalts were matched by shifting the curves (plotted on transparent paper) both horizontally and vertically for coincidence in shape. Upon finding
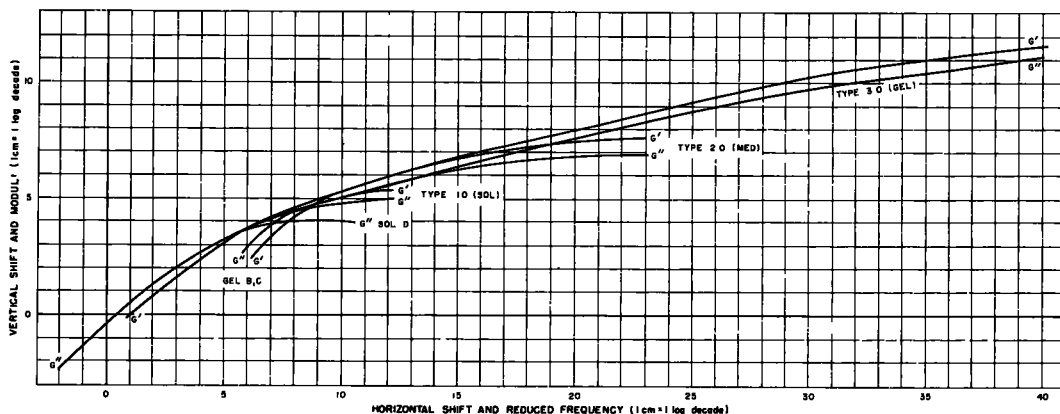
MASTER CURVES FOR NARC TYPE ASPHALTS

Figure 5. Master curves for NARC type asphalts.

coincidence in shape, the temperature which matches the point $T - T_S$ equal to zero on the log a_T versus T plot would be the T_S value. The reference temperatures, T_S, found are listed in Table 4 and it is seen that the softening points in degrees centigrade are very similar in value to those reference temperatures. Figure 7 shows that all the asphalts form one curve from $T - T_S$ equal to zero to $T - T_S$ equal to 150 C, but below $T - T_S$ equal to zero one has three distinct curves. The curves can be differentiated by using the penetration values at 77 F. The upper curve holds for the NARC asphalts with a penetration greater than 30 decimillimeters for 5 sec under a load of 100 g. The lower curve holds for a penetration of less than 15 decimillimeters under the same conditions. The middle curve holds for values of penetration between 15 and 30 decimillimeters.

Water Permeability of Asphalt

Although asphaltic materials have been used for a long time as barriers to hold back moisture, it is known that these materials have measurable permeabilities to water vapor and other gases.

The permeability measurements reported here were made by using the procedures developed by Beckman et al (15) but with a slightly modified apparatus. The data obtained at 99.5 and 77.8 F are given in Table 5. The diffusion constants do not vary as would be expected from viscosity and asphalt-water interfacial tension information. There is an indication that the results might correlate with the polarity or unsaturation
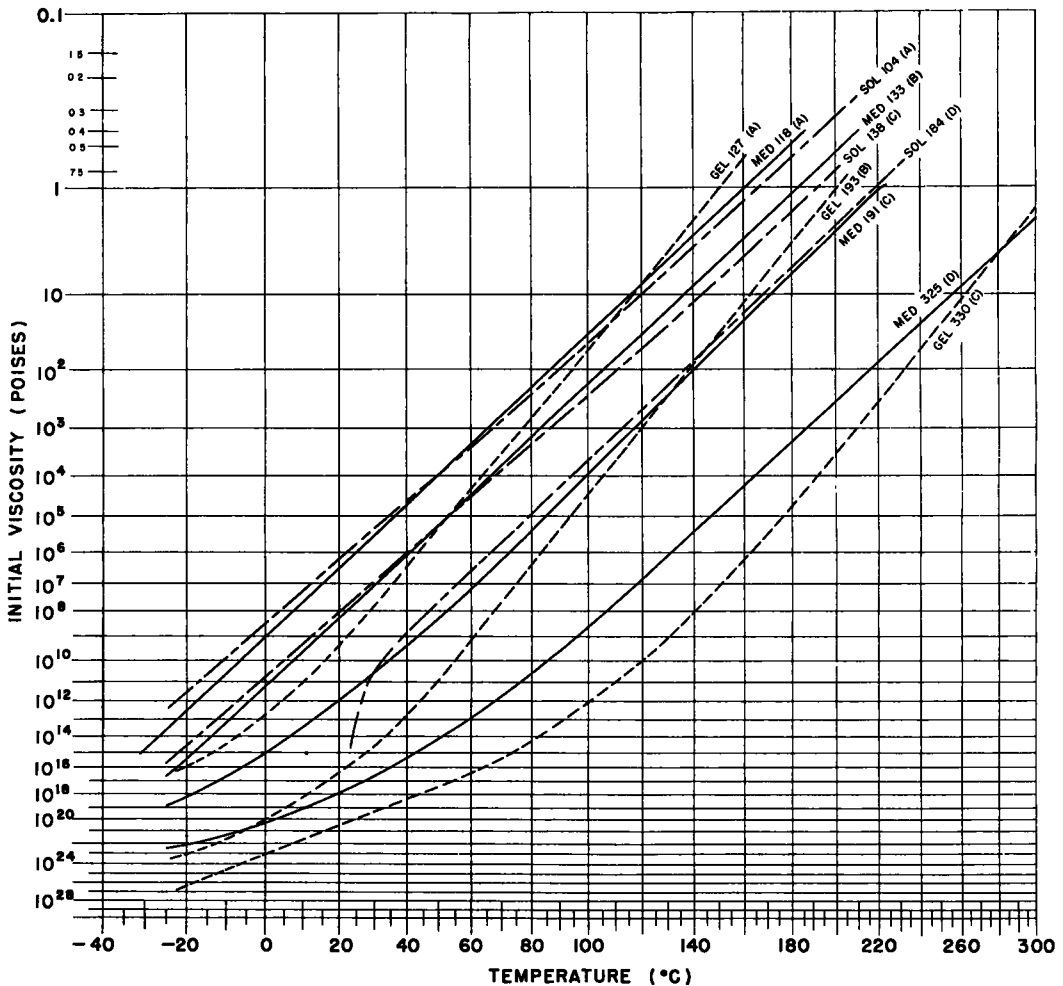
Figure 6. Initial viscosity of all NARC asphalts.

of the asphalts, which increases as they are airblown. The lesser diffusion at 77.8 F as compared with 99.5 F is believed to be due to the greater kinetic energy of the water vapor molecules at the higher temperature.

This permeability has been determined by the use of Fick's Law giving:

$$W = DAP\ \tau/L$$

in which,

W	=	weight of water passing through the film, grams
D	=	diffusion constant
A	=	area of film, cm^2
P	=	vapor pressure difference across the film
τ	=	time, hours
L	=	length of diffusion of path, cm.

The driving force, or difference in free energy, of course was the difference in pressure in this case. The driving force may be given by some other thermodynamic unbalance, that is, chemical reaction, etc., but a similar type of equation should hold as long

as P is replaced by the new driving force. These driving forces are discussed in E. Thelen's paper under the diffusion of water molecules through asphalt (21).

Photochemical Decomposition

Weathering is a complex phenomenon which depends upon many fundamental properties. As a first step it was decided to investigate the effect of ultraviolet radiation on asphalt surfaces. It was known that the contact angle of water droplets on polymers decreases markedly after exposure to high intensity Hanovia ultraviolet arc lamp for only a few hours. Therefore, it was decided to follow any chemical change on the surface of the asphalt by measuring the change of the contact angle of water droplets.

Three different asphalts were exposed to ultraviolet light for increasing periods of time. The contact angle of water droplets on these surfaces did decrease with increasing periods (Fig. 8). In addition, there were some easily visible changes in the samples. Wrinkles, cracks and bloom occurred to a degree which increased with the length of exposure.

Miscellaneous Properties of Asphalts

Properties such as tackiness, fatigue, mar resistance, etc., are also of great interest to the engineer dealing with asphalt. Some work has been done on these properties but it is only of a preliminary nature. Tackiness, that is, the resistance of liquid adhesive joints to fail in cohesion,

Figure 7. Master plot of log a_T vs $T - T_s$ (NARC asphalts).

is determined by the rheology of the adhesives and is not affected by their adhesion to the substrates. In fact, the tack temperature as defined by McLaren, Rager and Mark (16) is the lowest temperature at which two polymer films fuse when under a pressure of 20 psi and is found experimentally to be a temperature of constant viscosity. Bekerman has found that if the adhesive is Newtonian, tackiness is governed by Stefan's equation $4S t \delta d^2 = 3 \eta r^2$; S is the applied stress, t time of separation, and d initial thickness of the liquid film, η its viscosity and r radius of the adhered plates used in the experiment.

There are indications (22) that fatigue resistance is enhanced by using materials with both higher storage moduli and higher tan δ. Here colloidal differences may be more important than rheological properties.

It is found that mar resistance is increased by using a material with a high storage modulus and a low viscosity. Here a thick film gives greater resistance.

CORRELATION WITH PRACTICAL TESTS

The practical tests mentioned throughout this paper are described in more detail here. The penetration (ASTM D946-47T) is defined as the depth, measured in multiples of 0.1 mm, that a standardized needle penetrates into an asphalt surface under a constant load (100 g) in a specified time (5 sec).

The softening point, (ASTM E28-42) ring and ball, is determined as follows. A ring of given dimensions, filled with asphalt, is loaded with a steel ball (3.5 g). The whole is heated in a bath and the temperature at which the asphalt reached a certain deformation is reported as the ring and ball softening point.

It has been found experimentally that a certain penetration corresponds to a certain complex modulus, G*, at a rate of shear of 2.5 sec^{-1} or a frequency of .40 cps. Therefore a plot of complex modulus versus penetration for a number of asphalts (Fig. 9) should give a straight line. The figure shows a line drawn from van der Poel's data with
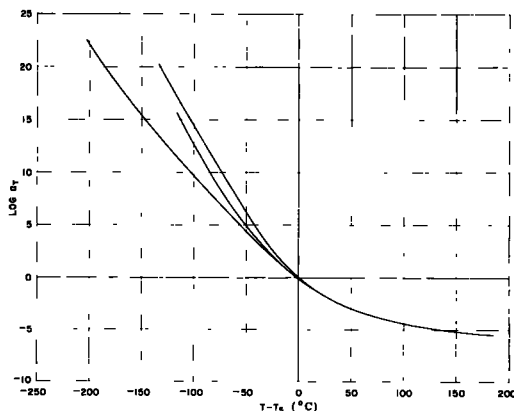
the points corresponding to the NARC standard asphalts. From these results, it can be seen that the determination of the penetration of an asphalt gives one a value of the complex modulus, G*, which is essentially an envelope of the G' and G" curves, at a frequency of 0.40 cps at 25 C (77 F).

PREDICTION OF RHEOLOGICAL BEHAVIOR FROM KNOWLEDGE OF THE SOFTENING POINT AND THE PENETRATION

The rheological properties of an asphalt are satisfactorily known if one has its reduced variable curves for G' and G" and its curve for initial viscosity as a function of temperature. Presented here is a means for obtaining a complete rheological description of an unknown asphalt, by running a minimum of laboratory measurements and utilizing the rheological curves for asphalts in general.

One first determines the softening point and penetration at 77 F, then looking at the figure (Fig. 1) for log penetration vs softening point the family in which the unknown asphalt belongs can be determined. Knowing this one knows which "section" of the generalized curve (Fig. 5) to use. Using again the softening point and penetration data and Figure 10, a vertical shift can be obtained which gives the point at which G' and G" are 10^6 dynes/cm^2 at 25 C, and a horizontal shift, which gives the point at which the frequency is one cycle per sec at 25 C. These shifts are measured from the origin (0, 0) on Figure 5 and the axes of these points should be labelled 10^6 and 1 cps respectively.

If it is assumed that the softening point is equivalent to T_S, one can determine the proper curve of log a_T vs temperature (Fig. 7). Therefore, one now has the reduced curves of G' and G" vs frequency and their temperature dependence.

As $\omega \eta$ = G" at the lowest frequencies, it is possible to determine the initial viscosity at 25 C from the generalized curve given above; the log a_T vs temperature curve and Eq. 2 can be used to determine the viscosity at any other temperature. In this manner an initial viscosity vs temperature plot can be drawn for the unknown asphalt.

It must be stressed that these correlations are empirical and are derived from tests on NARC asphalts only. However, a check may be made on the positioning by obtaining the value of the complex modulus at 0.4 c/s and 25 C from the penetration at 77 F and the figure of log complex modulus vs log penetration (Fig. 9) and determining if it is the same as predicted by the generalized curve.

Sol C which has a penetration of 32 at 77 F and a softening point of 137 F (58.4 C) can be taken as an example of this method. From Figure 1 it can be seen that here is a member of the Sol family. By interpolating between the lines of Figure 10 a vertical shift of 1.00 and a horizontal shift of 3.65 are obtained. Making these shifts on the generalized curve (Fig. 5) one obtains the points for G', G" = 10^6 dynes/cm^2 and f = 1 c/s. At 0.4 c/s this generalized curve predicts G* = 3 x 10^7 as determined from Eq. 10. Figure 8 predicts G* = 0.80 x 10^7 dynes/cm^2. This agreement is probably good enough for engineering work and really is a small error considering that the values of moduli may easily change by several orders
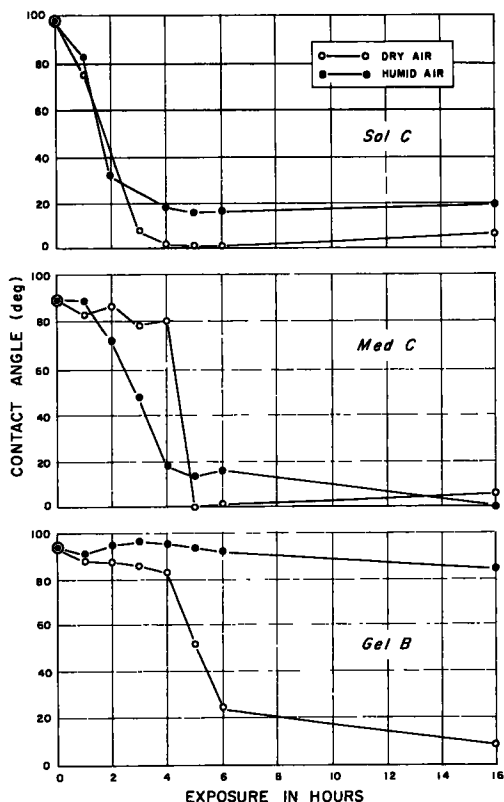

Figure 8. Effect of ultraviolet radiation on contact angles.

TABLE 4
CORRELATION OF T_S WITH SOFTENING
POINT

Code Name	T_S C	Softening Point C
Gel A	65.5	52.8
Gel B	106	89.5
Gel C	174	168.2
Med A	44	44.5
Med B	56	56.6
Med C	84	88.4
Med D	137	148.2
Sol A	34	38.9
Sol C	56	58.4
Sol D	86	84.5

TABLE 5
DIFFUSION CONSTANTS OF ASPHALTS
(Expressed in g/cm/mm Hg/hour x 10^9)

Code Name	99.5 F	77.8 F
Gel A	14.9	9.6
Gel B	17.4	---
Gel C	22.2	---
Med A	---	---
Med B	---	---
Med C	16.4	10.0
Med D	21.4	12.8
Sol A	---	---
Sol C	16.6	---
Sol D	---	---

of magnitude with temperature and frequency changes.

By extrapolating to the lowest frequencies, where G' disappears, it is found that the initial viscosity determined from the generalized curve is 2.52 x 10^7 poises. To determine the initial viscosity at 100 C the log a_T vs T curve can be used (Fig. 7) and it is found that the shift from 25 C to 100 C is -5.50 or a_T = 3.16 x 10^{-6}. As

$$\left(\frac{T_{100}\, \rho_{100}}{T_{25}\, \rho_{25}} \right) \simeq 1.20$$

Eq. 2 may be used to calculate the initial viscosity at 100 C. The Eq. $\frac{T \rho}{T_0 \rho_0} = 1+$ $(\frac{1}{T_0} - \alpha) \Delta T$ was used where α = 6.1 x 10^{-4}

$$\eta_{100} = a_T \left(\frac{T_{100}\, 100}{T_{25}\, T_{25}} \right) \quad \eta_{25} = 3.16 \times 10^{-6}$$

x 1.20 x 2.52 x 10^7 = 95.5 poises. This compares with the experimentally-determined value of 290 poises.

EXAMPLES OF USE OF RHEOLOGICAL DATA FOR ASPHALTS

After reduced variable curves for an unknown asphalt are obtained what can be done with them? Below are given a few examples of engineering questions which might be asked. The examples are selected to show the various aspects of asphalt behavior which may be ascertained from the data: (a) a flow problem, sliding on a slanted surface under the weight of granules; (b) damping, the attenuation of vibrations by asphalt; (c) a deformation problem, the bending of a beam under a concentrated load; and (d) a strength problem, the stresses set up by thermal change.

In the first example it is necessary to know the initial viscosities of the asphalts. In the second example the ratio of the loss modulus to the complex modulus is the determining quantity. This shows the necessity for separating the complex modulus into its components. The third example uses the whole complex modulus and the fourth example uses the information on the breaking properties of asphalt.

Sliding of Granules on a Roof

Sliding of granules or other loads on slanted decks can be calculated readily by means of the parallel plate viscometer as a model. The asphalt is visualized as a layer between the felt and the granules. It is sheared by the vertical component of the granule weight.

$$\eta = \tau \frac{tl}{d}$$

where

d	=	amount of flow,
l	=	thickness of asphalt film.

$$\tau = \frac{W \sin\theta}{A}$$

when

W = weight of granules,

A = area of granules,

θ = pitch of the roof, and

t = time in sec.

As a practical problem the ASTM softening point and penetration of a Medium asphalt that will permit a slide rate (d/t) of 0.01 in. per month at 135 F under a weight of granules of 60 lb/100 ft^2 will be determined. The thickness of the asphalt is 0.05 in. and the pitch of the roof is 1:5.

$$\sin\theta = \frac{1}{\sqrt{1^2 \times 5^2}} = 0.196$$

$$\tau = \frac{W \sin\theta}{A} = \frac{60}{100 \times 144}\,(0.196) = 0.000818 \text{ psi} = 56.3 \text{ dynes/cm}^2$$

Since this value of τ is well under 3,000 dynes/cm^2, the asphalt will behave as a viscous liquid (Sec 3A), whose initial viscosity at 135 F is desired.

$$\eta = \tau\,\frac{tl}{d} = \frac{56.3 \times 2.59 \times 10^6 \times 0.05}{0.01} = 7.3 \times 10^8 \text{ poises}$$

From Figure 6 it is known that the asphalts have these initial viscosities:

MED C, 191 SP = 2.9×10^7 poises, and
MED D, 325 SP = 1.8×10^{13} poises.

For a fair approximation the log of the initial viscosities vs the softening point is plotted. This relationship is approximately linear. Then by interpolation the softening point is found for which $\eta = 7.3 \times 10^8$. It is 224 F. From Figure 1 it is seen that the penetration is 11.3.

In passing it is noted that both the thickness of the asphalt layer and the weight of the granules enter directly into the calculations as first powers; doubling the thickness or doubling the weight of granules would also double the creep rate and double the required viscosity.

Attenuation of Vibrations

The basic manifestation of the absorption or attenuation of vibrational energy is the conversion of organized systematic motions of the particles of the medium into the uncoordinated random motions of thermal agitation. If it is assumed that the organized motion is sinusoidal and has the angular frequency $\omega = 2\pi f$, the velocity of a surface causing a shearing motion can be represented by
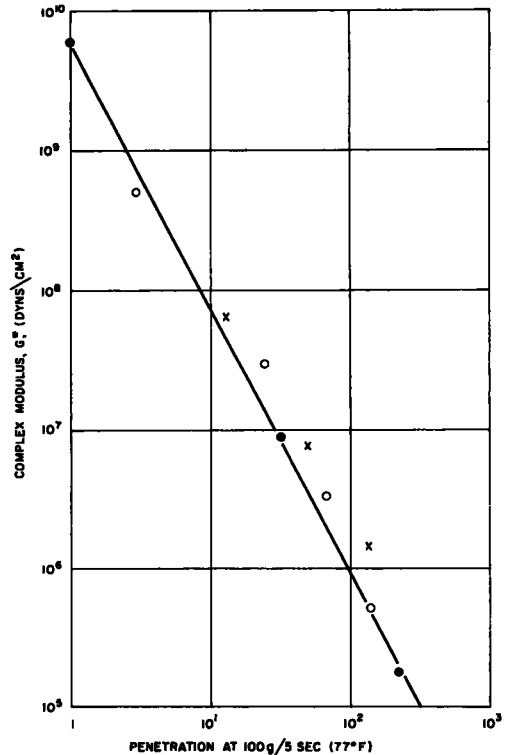
$$v_s = v_0 e^{i\omega t}$$

Figure 9. Relation between complex modulus at f = 0.4 cps and penetration at 5 sec.
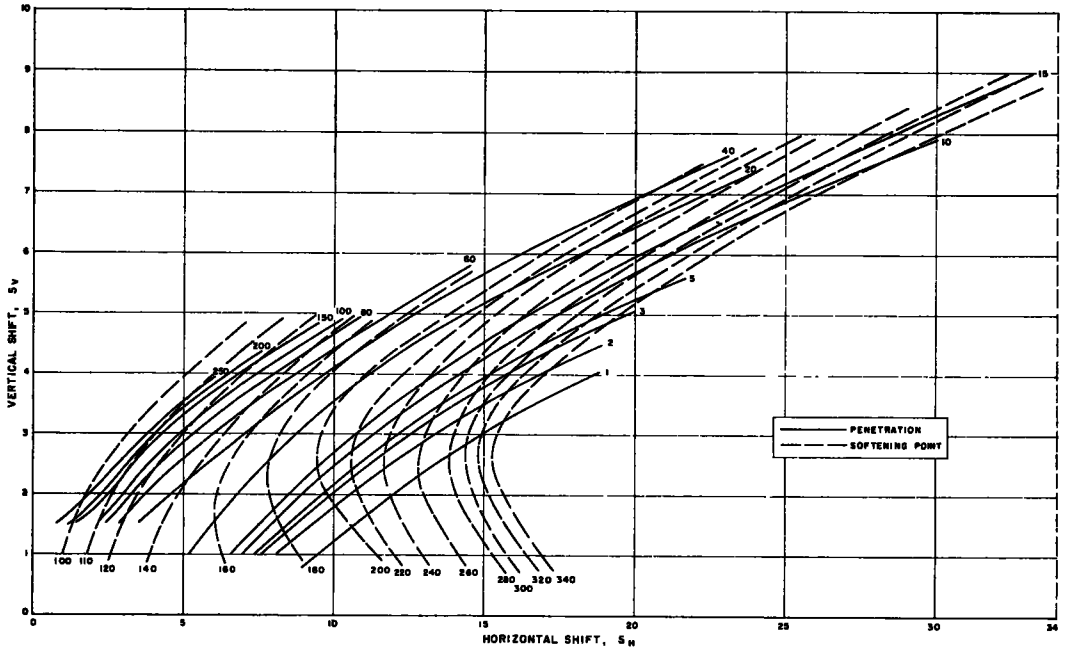
Figure 10. Relationship between horizontal and vertical shifts for given softening point and penetration (basis: 10 asphalts).

The transverse velocity of the liquid at the distance x from the oscillating surface is:

$$v_1 \quad = \quad v_0 e^{-\Gamma x} e^{i\omega t}$$

where Γ is the complex propagation constant, $\Gamma = (i\omega\rho / \eta*)^{\frac{1}{2}}$

$$i \quad = \quad \sqrt{-1}$$

ρ is the density, and

$\eta*$ is the complex viscosity defined as $\eta* = \eta' - i\eta''$

$$\eta' \quad = \quad \frac{G''}{\omega} \quad \text{and} \quad \eta'' = \frac{G'}{\omega}$$

Therefore if it is assumed that $\Gamma = \alpha + i\beta$, that is,

$$v_1 \quad = \quad v_0 e^{-\alpha x} e^{i(\omega t - \beta x)}$$

$$\Gamma^2 \quad = \quad \alpha^2 - \beta^2 + 2\alpha\beta i \quad = \quad \frac{i\omega\rho}{\eta' - i\eta''}$$

By suitable algebraic manipulation

$$\alpha \quad = \quad \frac{\omega\rho^{\frac{1}{2}} G''}{|G*| (G' + |G*|)^{\frac{1}{2}} (2)^{\frac{1}{2}}} \quad \text{and} \quad \beta \quad = \quad \frac{\omega\rho^{\frac{1}{2}} (G' + |G*|)^{\frac{1}{2}}}{|G*| (2)^{\frac{1}{2}}}$$

α is the attenuation constant and measures the rate at which the wave is damped or attenuated. It can be seen that at a given frequency the attenuation is essentially dependent on the ratio $G''/|G*|^{3/2}$. Therefore for rapid attenuation it is imperative to have a large value of G'' with respect to $|G*|$, that is, $G'' >> G'$. To transmit energy with little attenuation it would be necessary to have $G'' << G'$.

As an attenuation constant, α measures the rate at which energy is dissipated. Actually, vibration is not always caused by a shearing wave. For example the impact of an

object on the surface of an asphalt highway surface would send a compressional wave through the material but it would be attenuated in qualitatively the same manner as a shearing wave. Therefore it may not be possible to tell quantitatively the exact amount of attenuation of a wave, but asphalts can be compared and it is known that the one with the larger ratio of G'' to $|G*|^{3/2}$ will dissipate energy faster.

Use of Results of Classical Elastic Theory

Once the properties of a visco-elastic material have been described, there still remains the problem of the behavior of visco-elastic objects in which the stress and strain are functions of both position and time. The bending of a beam under a concentrated load at the center is taken as an example. The classical elastic law (18) gives

$$\frac{\partial^2 \xi}{\partial x^2} = \frac{-M_B}{EI} \tag{1}$$

where

ξ = deflection of the beam at a distance x from the support on one side,

M = moment causing the deflection,

E = Young's Modulus,

I = moment of inertia.

For a visco-elastic body, ξ, E and M are also functions of time;

$$E^*(t) I \frac{\partial^2 \xi(x,t)}{\partial x^2} = -M_B(x,t) \tag{2}$$

The differential equation can be solved using the well-known method of separation of variables. Therefore, $\xi(x,t) = X(x) T(t)$ is assumed and $-M_B(x,t) = g(x) f(t)$ and one obtains:

$$E^*(t) I \frac{d^2 X(x)}{dx^2} T(t) = g(x) f(t) \tag{3}$$

Collecting like terms on opposite sides of the equal sign and equating them to a constant (1/k) one obtains:

$$I k \frac{d^2 X(x)}{dx^2} = g(x) \tag{4a}$$

$$E^*(\omega) T(t) = kf(t) \tag{4b}$$

Under these conditions it is seen that the visco-elastic problem leads to a space equation that is identical with that obtained in the pure elastic problem, with k acting as the modulus of elasticity. Consequently, its solution is known.

$$X(x) = \frac{PL^3}{kbh^3} \left(\frac{3x}{4L} - \frac{x^3}{L^3} \right) \tag{5}$$

and as $\xi(x,t) = X(x) T(t)$,

$$\xi(x,t) = \frac{L^3}{bh^3} \left(\frac{3x}{4L} - \frac{x^3}{L^3} \right) \frac{Pf(t)}{E^*(\omega)} \tag{6}$$

Here the classical Young's Modulus is replaced by the complex modulus and the term gives the time dependence of the stress. The maximum stress and deformation are given by the equations:

$$\sigma_{max}(t) = \frac{3}{2} \frac{L}{bh^2} Pf(t) \tag{7}$$

and

$$\xi_{max}(x,t) = \frac{L^2 \rho(t)}{6hE^*(\omega)} \quad \text{or} \quad \xi_{max}(x,t) = \frac{L^2}{6h} Y(t) \tag{8}$$

If the application of stress is sinusoidal, then $\sigma(t) = \sigma_0 \sin \omega t$, or

$$\xi(x,t)_{max} = \frac{L^2 \sigma_0 \sin \omega t}{6hE^*(\omega)} \tag{9}$$

However, if a constant stress is applied, then σ_{max} is not a function of time, that is,

$$\sigma_{max} = \frac{3L}{2bh^2} P$$

In this problem it may be desired to know the deformation after a given time. The strain will be determined by the equation (20)

$$Y = \left[\epsilon_\infty + t/\eta + \psi(t)\right]\sigma \tag{10}$$

$\sigma \epsilon_\infty$ is the instantaneous component of strain and, being quite small, may be neglected; η is taken to be the initial viscosity if σ is less than 3,000 dynes/cm^2 and $\psi(t)$ is the creep function with $\psi(0) = 0$. In this particular case,

$$\xi(x,t)_{max} = \frac{L^2}{6h} Y(t)$$

thus

$$\xi(x,t)_{max} = \frac{L^2}{6h}\left[t/\eta + \psi(t)\right]\sigma$$

governs the flow or deformation of a beam at the point of concentrated load. To determine $\psi(t)\sigma$ from the basic data of G' and G'' vs f is a matter of graphical evaluation.

First to be determined is what is known as the relaxation distribution function, Φ, as a function of relaxation time, τ. If it is assumed that $\tau = 1/\omega$ where $\omega = 2\pi f$ for each evaluation, Φ is given approximately by the following equations (9):

$$\Phi(-\ln \omega) = G' \frac{d \log G'}{d \log \omega} \tag{11a}$$

$$\Phi(-\ln \omega) = G''\left(1 - \frac{d \log G''}{d \log \omega}\right) \tag{11b}$$

This function then can be determined from the family curves. The Φ vs τ curves for the NARC asphalts are given in Figure 11. Ferry et al have shown that the course of stress relaxation after cessation of steady flow, the author's $\psi(t)\sigma$, is given approximately by

$$\dot{Y} \int_{\ln t}^{\infty} \tau \Phi \, d \ln \tau$$

where $\dot{Y}$ is the rate of shear strain and it may be approximated by σ/η.

If $\tau \Phi$ vs $\log \tau$ is plotted and if one evaluates graphically from $\log t$ to infinity, $\psi(t)\sigma$ can be obtained; therefore, the deformation under a constant concentrated load, such as the wheel of a parked car can be obtained.

In this example several noteworthy features of general nature are seen. The complete space and time dependent problem splits neatly into one spatial problem and one temporal problem. The spatial problem is identical with that for a purely elastic problem and the temporal one may be solved with the knowledge of the time behavior of the elastic moduli.

This method of attack may be used on many problems, such as the deflection of an asphalt road bed under passing cars, rutting, shoving, etc.

Thermal Stresses

When the temperature of an unrestrained body is increased by ΔT, dilation of an amount proportional to ΔT can be produced without any corresponding change of pressure. This implies extension of all linear elements by $\alpha \Delta T$, where α is a constant, the coefficient of linear expansion. If forces are applied to the body, the strain at a point consists of such extension superposed upon a strain connected with the stress by the usual stress-strain equations.

According to these assumptions the stress, (σ) and strain in a body strained by change of temperature do not obey Hooke's Law, but are connected by the equation:

$$\gamma \text{ (tensile strain)} = \alpha \, \Delta T - \frac{\sigma \text{ (tensile)}}{E}.$$

If the asphalt is constrained so that it cannot move, that is, $\gamma = 0$ then a compressive stress is created which is equal and opposite to $\alpha \, \Delta TE$.

As $\alpha = 2.0 \times 10^{-4}$ (24) and $E \sim 3G'$ if incompressibility is assumed a relationship between the change in temperature and a compressive stress is obtained.

Therefore $\sigma = 6.0 \times 10^{-4} \, G' \Delta T$ and this stress must be below the breaking stress if a crack-free continuum is to exist. As the temperature change must be measured in a finite time and both G' and the breaking stresses are dependent on time, the rate at which the temperature changes is very important. For slow changes, except at very low temperatures, the stresses are low and should be able to relax with the loss mechanisms coming into play. However with rapid changes of temperature G' will be of the order of 10^9 to 10^{10} dynes/cm^2 and $\sigma = 6.0 \times 10^5 \Delta T$ to $6.0 \times 10^6 \Delta T$. In the section on breaking strength it was shown that the breaking stresses vary from 0.7×10^7 to 2.4×10^7 dynes/cm^2 at high rates. Therefore one must have $(6.0 \times 10^5$ to $6.0 \times 10^6) \Delta T < 0.7 - 2.4 \times 10^7$. This means that it might be possible to have a change of 100 C without any cracks.

The results depend upon the equation

$$6.0 \times 10^{-4} \Delta T < \frac{\sigma}{G'} \text{ Breaking}$$

where ΔT is the temperature change which takes place during the time of the experiment. This shows that the change in temperature a material can take depends upon the ratio of the breaking stress to the storage modulus. Therefore materials must be sought which have high breaking strengths and comparatively low moduli.

Figure 11. Distribution of relaxation times (all NARC asphalts).

CONCLUSIONS

All the foregoing information, the dependence of the moduli, G' and G'', on frequency, the temperature dependence of the asphalts, ets., show that asphalts behave very much like concentrated solutions of high polymers, that is, typical visco-elastic bodies. Therefore it has been possible to incorporate much of the work, both theoretical and experimental, in the high polymer field into the framework of an asphalt technology. It has then been possible to condense all the experimental information into a few
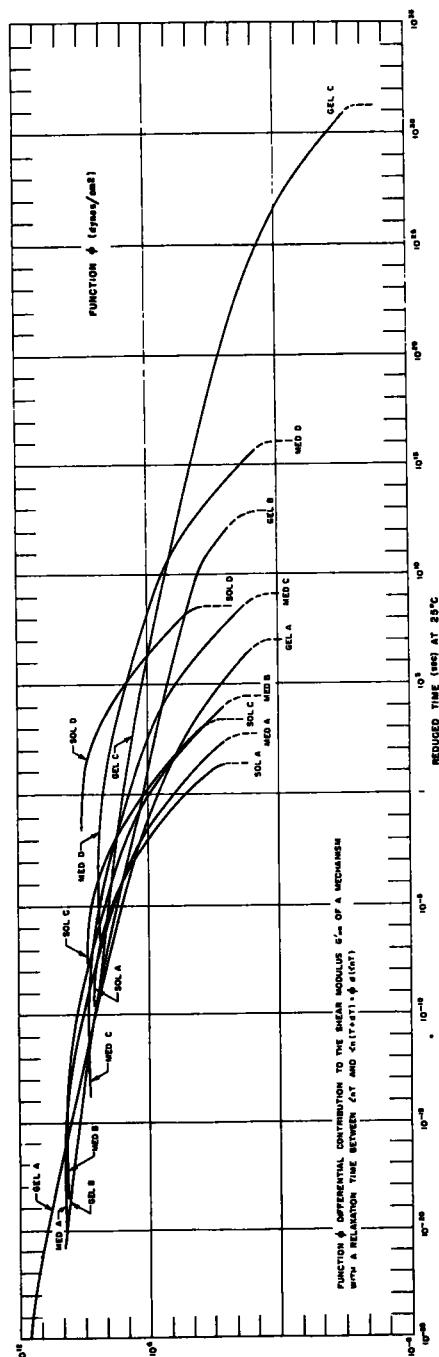
curves and tables: the family curves of moduli vs frequency, the curves showing the dependence of $\log a_T$ on $T - T_S'$ the dependence of initial viscosity on temperature, etc. These are essentially convenient methods for representing a great number of experimental results. If more data become available, changes may be required but major changes are unlikely as such a wide variety of types have been investigated.

With the calculation of the parameters involved in the two typical asphalt tests, softening point and penetration, it is possible now to decide in which family a particular asphalt belongs, its temperature dependence and its moduli dependence on frequency, and finally the dependence of its initial viscosity on temperature. Therefore from these two simple tests it is possible to find the whole rheological behavior of an asphalt, provided the generalized asphalt curves are available.

In the work just described the macroscopic behavior of asphalt has been investigated. No correlations with molecular structure are indicated but this is the ultimate aim of the physicist or chemist. Some work, not reported here, has been done in an attempt to relate empirically various portions of the relaxation spectra (Φ vs $\log \tau$) to various components of asphalt. Although partially successful more information is needed to extend the method. Possibly the new technique of Nuclear Magnetic Resonance might be helpful. An attempt, by the author, also not reported here, was made to estimate the molecular weights of the large particles involved in the flow of asphalt from the dynamic behavior of asphalt and present-day theories on the dynamic behavior of high polymers. The results indicated very large molecular weights for the flow particles. These are only initial attacks on the molecular basis of asphalt behavior and have yet to be followed up in detail.

The test on which the experimental results are based were made on freshly-poured asphalts. Therefore not much can be said about the change of the rheological behavior with aging. These aging properties are tied up with molecular motions and orientations which occur during application and service. Here again the new technique of Nuclear Magnetic Resonance may be able to show what changes take place.

It is hoped that this paper, which gives details on how asphalts react in flow, stimulates further work to answer why asphalts react the way they do.

ACKNOWLEDGMENTS

REFERENCES

1. Philippoff, W., Presented at Dallas meeting of the Amer. Chem. Soc. (To be published).
2. van der Poel, C., Proc. Int. Congr. Rheol. (No. 2 Oxford), p. 331. Butterworths Sci. Publ., London (1954).
3. van der Poel, C., Jour. Appl. Chem., 4:221 (1954).
4. van der Poel, C., Jour. Soc. of Plastics Eng., 11:47 (Sept. 1955).
5. Rostler, F.S. and Sternberg, H.W., Ind. Eng. Chem., 41:598 (1949).
6. Philippoff, W. and Gaskins, F.H., Jour. Polymer Sci., 21:205 (1956).
7. Philippoff, W., Gaskins, F.H. and Brodnyan, J.G., Jour. Appl. Physics. (To be published). (Oct. 1957).
8. Philippoff, W., Jour. Appl. Physics, 25:1102 (1954).
9. Ferry, Fitzgerald, Grandine and Williams, Ind. Eng. Chem., 44:708 (1952).
10. Philippoff, Sittel, Ferry and Plazek, Jour. Soc. of Plastics Eng., 11:41 (Sept. 1955).
11. Nielsen, Wall and Richmond, Jour. Soc. of Plastics Eng., 11:22 (Sept. 1955).
12. Mack, C., Ind. Eng. Chem., 44:422 (1957).

13. Smith, T.L., Fall 1956 meeting of the Society of Rheology.
14. Williams, Landel and Ferry., Jour. Am. Chem. Soc., 77:3701 (1955).
15. Beckman, Ind. Eng. Chem., 33:984 (1941).
16. McLaren, Rager and Mark, Jour. Polymer Sci., 7:463 (1951).
17. Bikerman, J.J., Trans. Soc. Rheol., 1:3 (1957).
18. Reiner, M., "Deformation and Flow," H.K. Lewis and Co. Ltd., London.
19. "Hutte," Band I p.665, Published by W. Ernst and Son, Berlin (1941).
20. Gross, B., "Theories of Visco-elasticity," Hermann and Co., Editors, Paris.
21. Thelen, E., "Surface Energy and Adhesion Properties in Asphalt-Aggregate Systems," Presented at Hwy. Research Bd. meeting, Jan. 6-10, 1958.
22. Thelen, E., Proc. Assn. Asphalt Paving Tech., 18:154 (1949).
23. Thelen, E., Private communication.
24. Pfeiffer, J., "The Properties of Asphaltic Bitumen," Elsevier Publ. Co., New York (1950).